

Concerted C–N and C–H Bond Formation in a Magnesium-Catalyzed Hydroamination

James F. Dunne, D. Bruce Fulton, Arkady Ellern, and Aaron D. Sadow*

Department of Chemistry and U.S. Department of Energy Ames Laboratory, Iowa State University, Ames, Iowa 50011, United States

Received October 1, 2010; E-mail: sadow@iastate.edu

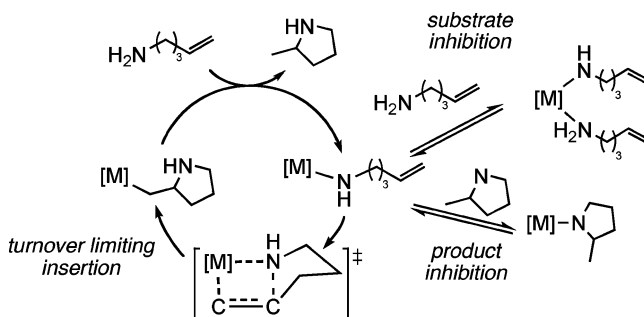
Abstract: Coordinatively saturated $\text{To}^{\text{M}}\text{MgMe}$ (**1**; To^{M} = tris(4,4-dimethyl-2-oxazolanyl)phenylborate) is an active precatalyst for intramolecular hydroamination/cyclization at 50 °C. The empirical rate law of $-\text{d}[\text{substrate}]/\text{dt} = k_{\text{obs}}[\text{Mg}]^1[\text{substrate}]^1$ and Michaelis–Menten-type kinetics are consistent with a mechanism involving reversible catalyst–substrate association prior to cyclization. The resting state of the catalyst, $\text{To}^{\text{M}}\text{MgNHCH}_2\text{CH}_2\text{CH}_2\text{CH}=\text{CH}_2$ [$\text{R} = \text{Ph}, \text{Me}, -(\text{CH}_2)_5-$], is isolable, but isolated magnesium amidoalkene does not undergo unimolecular cyclization at 50 °C. However, addition of trace amounts of substrate allows cyclization to occur. Therefore, we propose a two-substrate, six-center transition state involving concerted C–N bond formation and N–H bond cleavage as the turnover-limiting step of the catalytic cycle.

Migratory insertion of an olefin into a metal–nitrogen bond is exemplified by d^0 and f^0d^0 metal complex-catalyzed hydroamination/cyclization of aminoalkenes.¹ However, kinetic studies of these catalytic hydroaminations only provide indirect access to the proposed insertion step. The typical empirical rate law, $-\text{d}[\text{substrate}]/\text{dt} = k_{\text{obs}}[\text{catalyst}]^1[\text{substrate}]^0$, is interpreted as proceeding through turnover-limiting intramolecular insertion (Scheme 1).² In most cases this simplifies the overall mechanism because k_{obs} is a combination of elementary rate and equilibrium constants, and the observed rate constant often includes competitive association and/or substitution by product and substrate (i.e., inhibition).³ This amine substrate coordination may be mechanistically significant, as at least one additional amine is typically present in the catalyst resting state.^{2,3} Additionally, $k_{\text{H}}/k_{\text{D}}$ values ranging from 2 to 5 for H_2NR vs D_2NR substrates suggest that N–H bond cleavage is also involved in the rate-determining step and that C–N bond formation is more complicated than classical 1,2-insertion.^{3,4}

Furthermore, 1,2-insertion reactions between alkenes and $[\text{M}]-\text{NR}_2$ bonds that afford isolable metal alkyl compounds are rare. Group 4 examples are limited to alkyne insertions that provide vinyl amine products,⁵ as does the sole group 6 example.⁶ Activated olefins, such as norbornylene and acrylonitrile, react with amido-iridium(III) and amido-platinum(II) compounds, respectively, and these steps are useful in intermolecular hydroaminations.^{7,8} Recently, palladium amido compounds were shown to react through intramolecular and intermolecular olefin insertion pathways.⁹ We are not aware of stoichiometric insertion reactions of d^0 or f^0d^0 metal amides and alkenes that yield isolable metal alkyls. Despite the limited stoichiometric examples, a wealth of data and computational models have supported the general insertion mechanism for rare earth metal-catalyzed hydroamination (Scheme 1).¹⁰

To study the insertion step in hydroamination/cyclization, we decided to investigate catalysts in which bonding of an additional substrate might be limited by coordinative saturation. Tris(4,4-

Scheme 1. General Proposed Insertion Mechanism for Intramolecular Hydroamination



dimethyl-2-oxazolanyl)phenylborato [To^{M}] magnesium(II) compounds were chosen to provide the desired catalytic activity and steric properties, based on recent reports of the first examples of magnesium(II)- and calcium(II)-catalyzed intramolecular hydroamination¹¹ as well as extensive investigations of tris(pyrazolyl)borate magnesium compounds.¹² We have found that four-coordinate magnesium alkyl compounds are precatalysts for hydroamination/cyclization. Surprisingly, isolable magnesium amidoalkene complexes are not kinetically competent for intramolecular cyclization in the absence of additional aminoalkene. From this observation and the catalytic rate law, we propose an alternative pathway that invokes concerted C–N and C–H bond formation through a six-centered transition state.

$\text{To}^{\text{M}}\text{MgMe}$ (**1**) is prepared from HTo^{M} and $\text{MgMe}_2(\text{O}_2\text{C}_4\text{H}_8)_2$.¹³ A crosspeak between the oxazoline nitrogen and the $\text{Mg}-\text{CH}_3$ in a $^1\text{H}-^{15}\text{N}$ HMBC experiment demonstrates that **1** is the desired heteroleptic rather than a mixture of To_2Mg (**2**) and MgMe_2 . Neither THF nor dioxane coordinates to the magnesium(II) center in **1**, and no change in the ^1H NMR spectrum is detected upon thermolysis in benzene- d_6 at 150 °C in a sealed NMR tube. An X-ray structure of **1** (Figure 1) and solid angle determination show that 75% of the space surrounding the $\text{Mg}(\text{II})$ center is occupied by the To^{M} (60%) and CH_3 (15%) ligands.¹⁴

Compound **1** is a catalyst for the cyclization of primary 4-aminoalkenes (**3–5**) and a secondary aminoalkene (**6**) affording pyrrolidines (**7–10**) at 50 °C in benzene (Table 1). 2,2-Disubstitution is required for cyclization to occur, and the unsubstituted 4-pentene-1-amine is not cyclized by **1** at 50 °C.

The lack of coordination of ethers to **1** suggests that there is no open site for olefin coordination prior to insertion. As this is uncommon for hydroamination catalysts, we were motivated to further investigate the cyclization mechanism. The concentration of substrate **3** was monitored over the course of the reaction, and plots of $\ln[\mathbf{3}]$ vs time are linear for >3 half-lives. A plot of k_{obs} vs $[\mathbf{1}]$ is linear giving the empirical rate law: $-\text{d}[\mathbf{3}]/\text{dt} = k'_{\text{obs}}[\mathbf{1}]^1[\mathbf{3}]^1$ ($k'^{(\text{H})}_{\text{obs}} = 6.9 \times 10^{-3} \text{ M}^{-1} \text{ s}^{-1}$). Second-order rate laws for

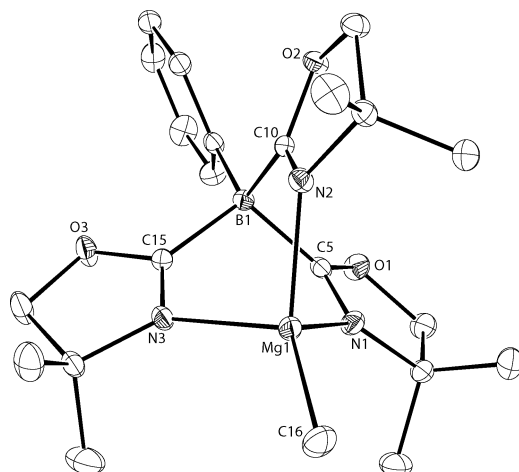


Figure 1. ORTEP diagram of To^{MgMe} (**1**). Selected bond lengths (Å): Mg1-N1 , 2.122(1); Mg1-N2 , 2.124(1); Mg1-N3 , 2.090(1); Mg1-C16 , 2.108(1).

Table 1. Hydroamination/Cyclization of Aminoalkenes Catalyzed by To^{MgMe} (**1**)^a

Entry	Substrate	Product	Time (h)	Conversion (%) ^b
1			12	99
2			72	20
3			15	99
4			48	99 ^c

^a Conditions: 10 mol % **1**, C_6D_6 , 50 °C. ^b Conversion (%) was determined by ^1H NMR spectroscopy. ^c 20 mol % **1**.

aminoalkene cyclization are uncommon, but a few examples have been reported.¹⁵ A plot of $k^{(\text{D})}_{\text{obs}}$ for cyclization of **3-d**₂ vs [**1**] gives $k^{(\text{D})}_{\text{obs}} = 1.5 \times 10^{-3} \text{ M}^{-1} \text{ s}^{-1}$. The ratio $k^{(\text{H})}_{\text{obs}}/k^{(\text{D})}_{\text{obs}}$ is 4.6, revealing a significant primary isotope effect. This rate law and isotope effect data are consistent with several possible mechanisms, including turnover limiting intermolecular protonolysis of a magnesium alkyl and a two-step sequence in which reversible catalyst–substrate association precedes unimolecular cyclization. If the reaction follows the latter pathway, the rate could show saturation at high aminoalkene concentrations.¹⁶ Indeed, ν_{ini} ($\nu_{\text{ini}} = -d[\mathbf{3}]/dt$ at 5% conversion) vs $[\mathbf{3}]_{\text{ini}}$ (Figure 2) increases until saturation is observed.

The catalyst $\text{To}^{\text{Mg}}\text{MgNHCH}_2\text{CPh}_2\text{CH}_2\text{CH}=\text{CH}_2$ (**12**) is preformed by reaction of $\text{To}^{\text{Mg}}\text{MgCH}_2\text{C}_6\text{Me}_2\text{H}_3$ (**11**) and **3** (see eq 4 below) prior to catalytic cyclization, and its concentration equals the measured concentration of $\text{C}_6\text{Me}_2\text{H}_3$. A nonlinear regression analysis correlates the data to eq 1.¹⁷

$$\frac{-d[\mathbf{3}]}{dt} = \frac{k_2[\mathbf{12}][\mathbf{3}]_{\text{ini}}}{K' + [\mathbf{3}]_{\text{ini}}} = \frac{k_2[\text{substrate}][\text{catalyst}]}{K' + [\text{substrate}]} \quad (1)$$

This rate law corresponds to the mechanistic sequence of eqs 2–3, where $k_2 = (1.4 \pm 0.2) \times 10^{-2} \text{ s}^{-1}$ (cyclization) and $K' = (k_{-1} + k_2)/k_1 = 0.24 \pm 0.05 \text{ M}$ (formation constant):

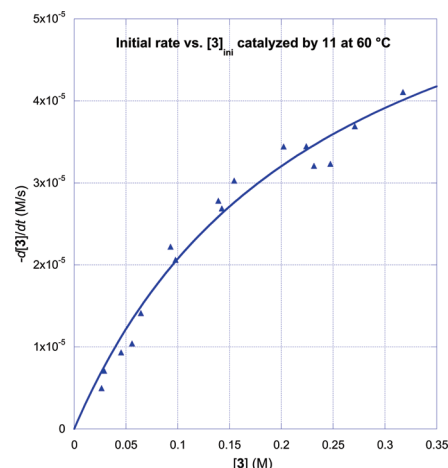
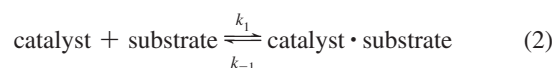
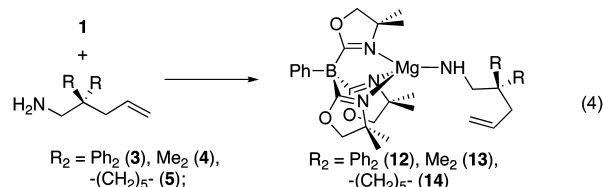


Figure 2. Plot showing relationship between initial rate $-d[\mathbf{3}]/dt$ and $[\mathbf{3}]_{\text{ini}}$ (Conditions: catalyst [**11**] = 0.00493 M, C_6D_6 , 60 °C). Each $-d[\mathbf{3}]/dt$ value is obtained from a linear-least-squares fit of $[\mathbf{3}]$ vs time for 5% conversion. The curve represents a nonlinear least-squares fit of the data to eq 1.

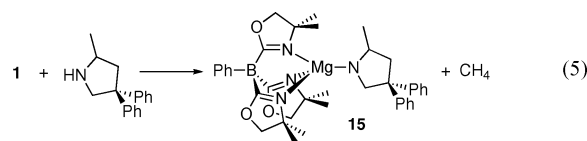


In contrast, turnover-limiting metal–alkyl protonolysis would be expected to show linear dependence on [substrate] over all concentrations.

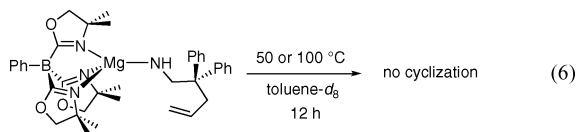
In order to better establish the nature of the cyclization step, the catalyst, and the catalyst·substrate intermediate, we investigated the identities of the species in the reaction mixture. Inspection of ^1H NMR spectra of catalytic reactions of a 10:1 ratio of substrate **3** to precatalyst **1** or **11** in benzene-*d*₆ reveals two To^{Mg} species. The first compound, **12**, was independently prepared in a stoichiometric reaction of **3** with the magnesium alkyls **1** or **11** (eq 4). Related magnesium amidoalkenes **13** and **14** are also formed upon treatment of **1** with the aminoalkenes **4** and **5**, and compounds **12**–**14** are isolated and fully characterized. Pseudo- C_{3v} symmetry of **12**–**14**, as indicated by ^1H and $^{13}\text{C}\{^1\text{H}\}$ NMR spectra and IR spectra (one ν_{CN} band), support the structure of eq 4 (see Supporting Information (SI)).



Previously, $\text{Cp}'_2\text{LaNHR}'(\text{NH}_2\text{R}')$ ($\text{R}' = \text{CH}_2\text{CMe}_2\text{CH}_2\text{CHCH}_2$) was characterized at low temperature but could not be isolated as cyclization occurs at ~ -20 °C.^{3a} Pyrrolide $\text{To}^{\text{Mg}}\text{Mg}(\text{NC}_4\text{H}_5-2\text{-Me}-4,4\text{-Ph}_2)$ (**15**) is the other To^{Mg} species present in the catalytic reaction mixture and is prepared by reaction of **1** and diphenylpyrrolidine **7** (eq 5).

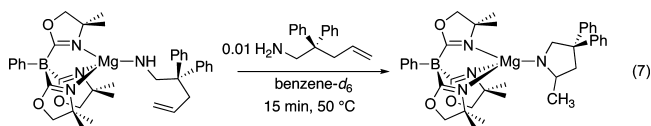


Magnesium amidoalkene **12** was observed in the catalytic reaction mixture, so its reactivity was tested by warming a benzene-*d*₆ solution of isolated **12** to 50 °C, and then 100 °C for 12 h (eq 6). Surprisingly, the amidoalkene was the only species observed under these conditions, and neither free pyrrolidine **6** nor magnesium pyrrolide **15** was formed.



This result contrasts the catalytic cyclizations where C–N bond formation occurs readily at 50 °C. Thus, the intermediate **12** is not kinetically competent to mediate olefin insertion on its own.¹⁸

Addition of a slight excess (≥ 1.01 equiv) of aminoalkene **3** to **1** provides **12** quantitatively after 15 min at rt. When this solution of **12** and 0.01 equiv of **3** is warmed to 50 °C, cyclization provides compound **15** (eq 7). These stoichiometric reactions and our kinetic measurements argue strongly that C–N bond formation occurs from an amine adduct of **12** (i.e., **12**·**3**) during catalysis.



Three-coordinate magnesium might be required for insertion.^{11b} In this scenario, eq 2 might involve amine-assisted dissociation of one oxazoline ring. Therefore $\text{To}^{\text{M}}_2\text{Mg}$ (**2**) was used to assess oxazoline-magnesium lability and the steric constraints imposed by the To^{M} ligand.

Homoleptic $\text{To}^{\text{M}}_2\text{Mg}$ contains two bidentate ligands. The magnesium center is coordinatively saturated and protected on all sides by the dimethyl groups of the oxazolines (Figure 3). This claim is supported quantitatively by crystallographic solid angles for **2**,^{14b–d} which are 5.70 and 5.77 steradians (45 and 46%), suggesting exchange (see below) involves oxazoline dissociation. This structural study further shows that an intramolecular insertion process in putative $\{\kappa^2\text{-To}^{\text{M}}\}\text{MgNHCH}_2\text{CR}_2\text{CH}_2\text{CH}=\text{CH}_2$ ($\sim 40\%$ free space) is not ruled out on steric grounds.

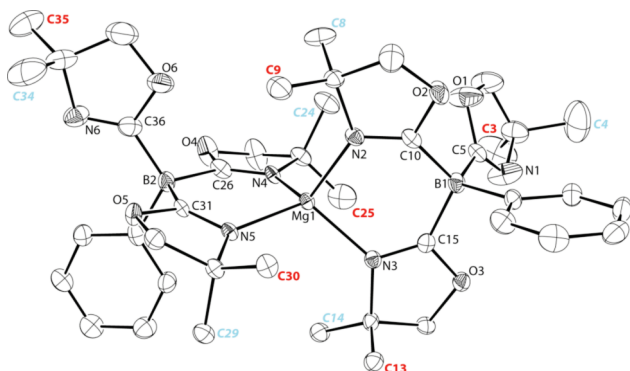


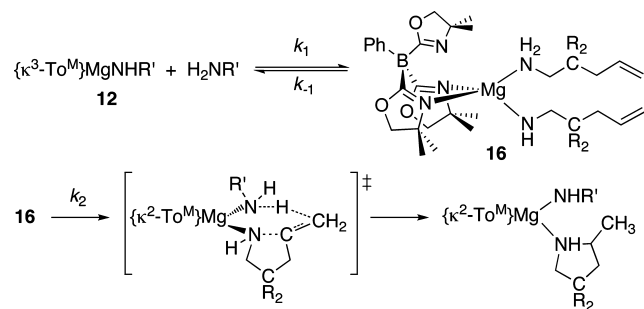
Figure 3. ORTEP diagram of $\text{To}^{\text{M}}_2\text{Mg}$ (**2**). Methyl groups that undergo chemical exchange are colored identically (bold red and blue italics). Selected bond lengths (Å): Mg1–N2, 2.063(4); Mg1–N3, 2.046(5); Mg1–N4, 2.070(5); Mg1–N5, 2.065(4).

An EXSY experiment at 50 °C showed selective exchange between methyl groups (C3, C9, and C13; C4, C8, and C14; see Figure 3) further supporting a dissociative rather than associative exchange mechanism. The rates of oxazoline exchange (35–72 °C;

benzene-*d*₆) were measured using selective population inversion (SPI).¹⁹ From this analysis, the rate of dissociative exchange (k_{diss}) at 60 °C is 0.20 s^{-1} , which is $\sim 14\times$ faster than k_2 (0.014 s^{-1}). Thus, the frequency of oxazoline dissociation is greater than the TOF for aminoalkene cyclization.

The oxazoline dissociation rate constants k_{diss} are likely similar in **2** and **12–14**.²⁰ Thus, an amine ligand is required for cyclization but not for oxazoline dissociation, suggesting that aminoalkenes **3–5** interact with the magnesium(II) center under catalytic conditions. The observations that (a) isolable compounds **12–14** do not undergo intramolecular cyclization, (b) a second substrate molecule is required for cyclization, and (c) the unobserved active species $\text{To}^{\text{M}}\text{MgNHR}'(\text{NH}_2\text{R}')$ (**16–18**; $\text{R}' = \text{CH}_2\text{CR}_2\text{CH}_2\text{CH}=\text{CH}_2$) are at least four-coordinate (i.e., coordination sites are limited) are not consistent with C–N bond formation via migratory insertion of the olefin into the Mg–N bond. Instead, we propose that C–N bond formation involves a six-center transition state as shown in Scheme 2. Related transition state structures, in which a proton is transferred from carbon to nitrogen, are proposed for ketone enolization by magnesium amides.²¹ Additionally, we have studied diamido zirconium(IV) hydroamination/cyclization catalysts where C–N bond formations appear to involve proton transfer from one amido to the terminal olefinic carbon in a related six-centered transition state.²²

Scheme 2. Proposed Mechanism for $\text{To}^{\text{M}}\text{Mg}$ -Mediated Aminoolefin Hydroamination^a



^a $\text{R}' = \text{CH}_2\text{CR}_2\text{CH}_2\text{CH}=\text{CH}_2$, $\text{R} = \text{Ph}_2$, $-(\text{CH}_2)_5-$, Me_2 .

Our kinetic studies and the reactivity of isolated magnesium amidoalkenes provide unambiguous evidence that two substrate molecules are interacting with the magnesium site in the turnover-limiting cyclization step. Coordinative saturation stabilizes the amine-free magnesium amido complex, affording a distinct and unique environment compared to other coordinatively unsaturated hydroamination/cyclization catalysts. Interestingly, the resting states of many d^0 and $f^0 d^0$ metal center hydroamination/cyclization catalysts, including lanthanidocenes,³ highly enantioselective binaphtholates compounds, and magnesium diketimines,¹¹ are amido-amine complexes $\{\text{L}_n\text{M}\}\text{-NHR}(\text{NH}_2\text{R})_n$, and the rate laws for these systems typically follow zero-order dependence on substrate concentration. Under saturation conditions, the rate law of eq 1 reduces to this commonly observed rate law, providing a possible connection between hydroaminations mediated by **1** and other d^0 -metal based catalysts. Despite this connection, the relative importance of the mechanism proposed in Scheme 2 with respect to insertion (or other) pathways remains to be investigated for catalysts with increased coordinative unsaturation.

Acknowledgment. We thank Dr. A. Bakac and Dr. K. Kristian for valuable mechanistic discussions. Mr. J. Engelkemier is thanked for preparation of **3-d**₂. The U.S. DOE Office of Basic Energy Science (DE-AC02-07CH11358) and the ACS Green Chemistry Institute-PRF provided financial support. James F. Dunne is

supported by a GAANN Fellowship. Aaron D. Sadow is an Alfred P. Sloan Fellow.

Note Added after ASAP Publication. Scheme 1 contained an error in the version published ASAP December 1, 2010; the correct version reposted December 15, 2010.

Supporting Information Available: Procedures and characterization data for compounds **1**, **2**, **11**–**15**, representative kinetic plots, and X-ray crystallographic data. This material is available free of charge via the Internet at <http://pubs.acs.org>.

References

- (1) (a) Hong, S.; Marks, T. J. *Acc. Chem. Res.* **2004**, *37*, 673–686. (b) Müller, T. E.; Hultsch, K. C.; Yus, M.; Foubelo, F.; Tada, M. *Chem. Rev.* **2008**, *108*, 3795–3892.
- (2) Gagne, M. R.; Marks, T. J. *J. Am. Chem. Soc.* **1989**, *111*, 4108–4109.
- (3) (a) Gagne, M. R.; Stern, C. L.; Marks, T. J. *J. Am. Chem. Soc.* **1992**, *114*, 275–294. (b) Gribkov, D. V.; Hultsch, K. C.; Hampel, F. *J. Am. Chem. Soc.* **2006**, *128*, 3748–3759.
- (4) Stubbert, B. D.; Marks, T. J. *J. Am. Chem. Soc.* **2007**, *129*, 6149–6167.
- (5) (a) Walsh, P. J.; Hollander, F. J.; Bergman, R. G. *J. Am. Chem. Soc.* **1990**, *112*, 894–896. (b) Leitch, D. C.; Turner, C. S.; Schafer, L. L. *Angew. Chem., Int. Ed.* **2010**, *49*, 6382–6386.
- (6) Katayev, E.; Li, Y.; Odom, A. L. *Chem. Commun.* **2002**, 838–839.
- (7) (a) Casalnuovo, A. L.; Calabrese, J. C.; Milstein, D. *J. Am. Chem. Soc.* **1988**, *110*, 6738–6744. (b) Dorta, R.; Egli, P.; Zürcher, F.; Togni, A. *J. Am. Chem. Soc.* **1997**, *119*, 10857–10858.
- (8) (a) Cowan, R. L.; Trogler, W. C. *Organometallics* **1987**, *6*, 2451–2453. (b) Cowan, R. L.; Trogler, W. C. *J. Am. Chem. Soc.* **1989**, *111*, 4750–4761. (c) Seligson, A. L.; Trogler, W. C. *Organometallics* **1993**, *12*, 744–751.
- (9) (a) Neukom, J. D.; Perch, N. S.; Wolfe, J. P. *J. Am. Chem. Soc.* **2010**, *132*, 6276–6277. (b) Hanley, P. S.; Markovic, D.; Hartwig, J. F. *J. Am. Chem. Soc.* **2010**, *132*, 6302–6303.
- (10) Motta, A.; Lanza, G.; Fragala, I. L.; Marks, T. J. *Organometallics* **2004**, *23*, 4097–4104.
- (11) (a) Crimmin, M. R.; Casely, I. J.; Hill, M. S. *J. Am. Chem. Soc.* **2005**, *127*, 2042–2043. (b) Crimmin, M. R.; Arrowsmith, M.; Barrett, A. G. M.; Casely, I. J.; Hill, M. S.; Procopiou, P. A. *J. Am. Chem. Soc.* **2009**, *131*, 9670–9685. (c) Horrillo-Martinez, P.; Hultsch, K. C. *Tetrahedron Lett.* **2009**, *50*, 2054–2056. (d) Neal, S. R.; Ellern, A.; Sadow, A. D. *J. Organomet. Chem.* **2010**, doi: 10.1016/j.jorganchem.2010.08.057.
- (12) (a) Han, R.; Looney, A.; Parkin, G. *J. Am. Chem. Soc.* **1989**, *111*, 7276–7278. (b) Han, R.; Parkin, G. *J. Am. Chem. Soc.* **1992**, *114*, 748–757. (c) Chisholm, M. H.; Eilerts, N. W.; Huffman, J. C.; Iyer, S. S.; Pacold, M.; Phomphrai, K. *J. Am. Chem. Soc.* **2000**, *122*, 11845–11854.
- (13) Dunne, J. F.; Su, J.; Ellern, A.; Sadow, A. D. *Organometallics* **2008**, *27*, 2399–2401.
- (14) (a) Solid angles of [To^M] and Me in To^MMgMe are 7.4 and 2 steradians, as determined by the program Solid-G using X-ray crystallographic coordinates. (b) White, D.; Coville, N. J. In *Advances in Organometallic Chemistry*; Academic Press: New York, 1994; Vol. 36, pp 95–158. (c) Guzei, I. A.; Wendt, M. *Dalton Trans.* **2006**, 3991–3999. (d) Guzei, I. A.; Wendt, M. *Solid-G*; UW-Madison, WI, USA, 2004.
- (15) (a) Hultsch, K. C.; Hampel, F.; Wagner, T. *Organometallics* **2004**, *23*, 2601–2612. (b) Thomson, R. K.; Bexrud, J. A.; Schafer, L. L. *Organometallics* **2006**, *25*, 4069–4071.
- (16) Espenson, J. H. *Chemical kinetics and reaction mechanisms*, 2nd ed.; McGraw-Hill: New York, 1995.
- (17) (a) See SI for kinetic analysis. (b) Cornish-Bowden, A. *Fundamentals of Enzyme Kinetics*, 3rd ed.; Portland Press: London, 2004; pp 137–141.
- (18) A referee suggested an alternative possibility for the apparent inert nature of **12**, where insertion is reversible but favors the magnesium-amido reactant. While this explanation cannot be ruled out for the stoichiometric reaction, the isotope effect and substrate saturation data, taken together, are not consistent with a reversible insertion under catalytic conditions.
- (19) (a) Bain, A. D.; Cramer, J. A. *J. Phys. Chem.* **1993**, *97*, 2884–2887. (b) Bain, A. D. *CIFIT*; Chemistry Department, McMaster University, 2003. (c) Kristian, K. E.; Iimura, M.; Cummings, S. A.; Norton, J. R.; Janak, K. E.; Pang, K. *Organometallics* **2009**, *28*, 493–498.
- (20) Mg–N bonds are highly polarized, and dissociation rates of Mg–N bonds in **1** and **11**–**13** are likely equal to or greater than rates for **2** based on Mg–N bond length and strain associated with κ^3 -coordination.
- (21) (a) Henderson, K. W.; Allan, J. F.; Kennedy, A. R. *Chem. Commun.* **1997**, 1149–1150. (b) He, X.; Morris, J. J.; Noll, B. C.; Brown, S. N.; Henderson, K. W. *J. Am. Chem. Soc.* **2006**, *128*, 13599–13610.
- (22) Manna, K.; Xu, S.; Sadow, A. D. *Angew. Chem., Int. Ed.*, accepted for publication.

JA108881S